Supporting Information

Hyaluronic Acid-based Hydrogels loaded with Chemoattractant and Anticancer Drug – new formulation for Attracting and Tackling Glioma Cells

Paraskevi M. Kasapidou[a,b*], Emmanuel Laillet de Montullé[b*], Kleouforo-Paul Dembélé[b], Alexandre Mutel[b],Laurence Desrues[b], Vladimir Gubala[a] and Hélène Castel[b†]

[a]Medway School of Pharmacy, University of Kent, Central Avenue, Chatham, ME4 4TB, United Kingdom

[b]Normandie Univ, UNIROUEN, INSERM U1239, DC2N, 76000 Rouen, France, Institute for Research and Innovation in Biomedicine (IRIB), 76000 Rouen, France

*Co-first authors

†Corresponding author: Hélène Castel, INSERM U1239, Laboratory of Neuronal and Neuroendocrine Cell Communication and Differentiation, Team Astrocytes and Vascular Niche, University of Rouen Normandie, 25 Rue Tesnière, 76821 Mont-Saint-Aignan, France.

E-mail address: helene.castel@univ-rouen.fr

Scanning electron microscopy

The microstructure of the hydrogels was evaluated using a FEG-SEM Hitachi SU8030 Scanning Electron Microscope. Prior to the SEM analysis, hydrogels were previously incubated in PBS for at least 24 h at 37 °C and subsequently frozen by immersion in dry ice. Frozen gels were then fractured with a scalpel and immediately placed on a lyophilizer for freeze drying. Hydrogels were affixed to a metal stub with carbon film and they were sputter-coated with a layer of gold for 2 minutes at 25 mA prior to observation using an Edwards Au coater. Several magnifications using accelerating voltage of 1.0 kV were obtained to study further the surface morphology and pore sizes of the hydrogels.

Fourier Transform Infrared Spectroscopy of HA-ADH hydrogels

FT-IR spectra of HA-ADH lyophilised hydrogels and their components were obtained using a Perkin Elmer Spectrum One FT-IR spectrometer equipped with a diamond universal attenuated total reflection unit. The spectra were obtained in the range of wavenumber from 4000 to 750 cm-1 by accumulating 16 scans. In Figure S1a, HA presents spectral characteristics typical for carboxylates anions, which are mainly absorption bands at 1607 and 1400 cm-1 assigned to the asymmetric and symmetric stretching vibrations of the carboxylate anions respectively. In the FT-IR spectrum of the HA-ADH lyophilised hydrogel, the main differences compared to that of the unmodified HA are the appearance of the characteristic peaks of the ADH modification at 1686 cm-1 which corresponds to the formation of the amide bond (C=O stretch of secondary amide) and 1558 cm-1 (N-H bend of amide). Moreover, in the HA-ADH spectrum, the absorption band at 2937 cm-1 represents the -CH2 stretching vibrations from the ADH moiety. In Figure S1b, it is noteworthy that the increasing concentration of the crosslinker did induce a slight increase in the intensity of the peaks as highlighted in the above graph corresponding to the formation of the amide bond at approximately 1680 and 1550 cm-1.

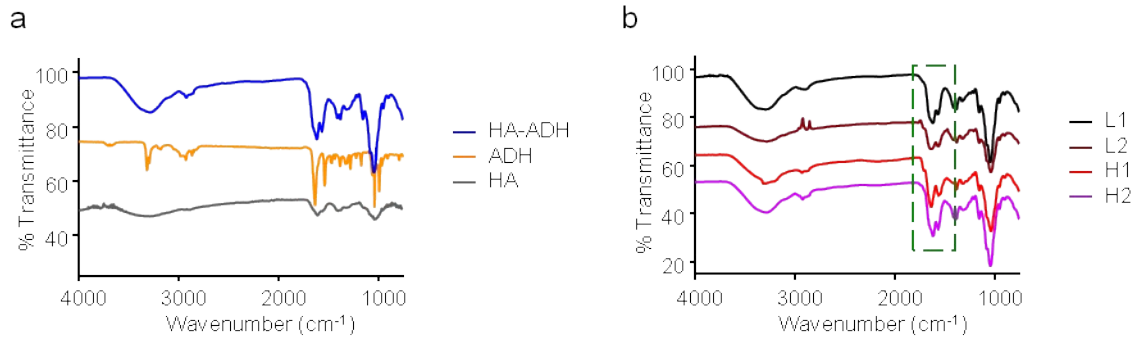

Fig. S1. a) FT-IR spectra of HA, ADH and HA-ADH lyophilized hydrogel. FT-IR spectroscopy was performed in order to investigate the structural changes of the prepared hydrogels compared with the structure of their precursor components. b) FT-IR spectra of HA-ADH lyophilized hydrogels prepared at different crosslinking densities.

In Figure S1b, it is noteworthy that the increasing concentration of the crosslinker did induce a slight increase in the intensity of the peaks as highlighted in the above graph corresponding to the formation of the amide bond at approximately 1680 and 1550 cm^{-1}.

UV-Vis absorbance/Calibration curve of DOX

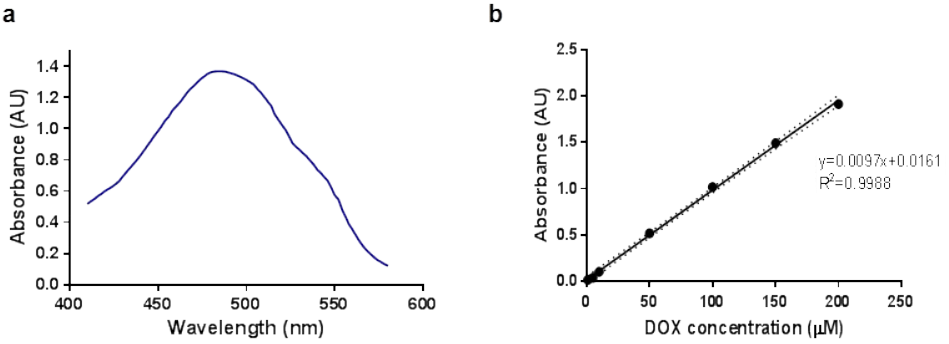

Fig. S2. a) UV/Vis spectrum of DOX, b) calibration curve of DOX in PBS (pH 7.4) obtained for the absorbance maximum (λ_{max}) of DOX solution.

UV-Vis absorbance/Calibration curve of TMZ

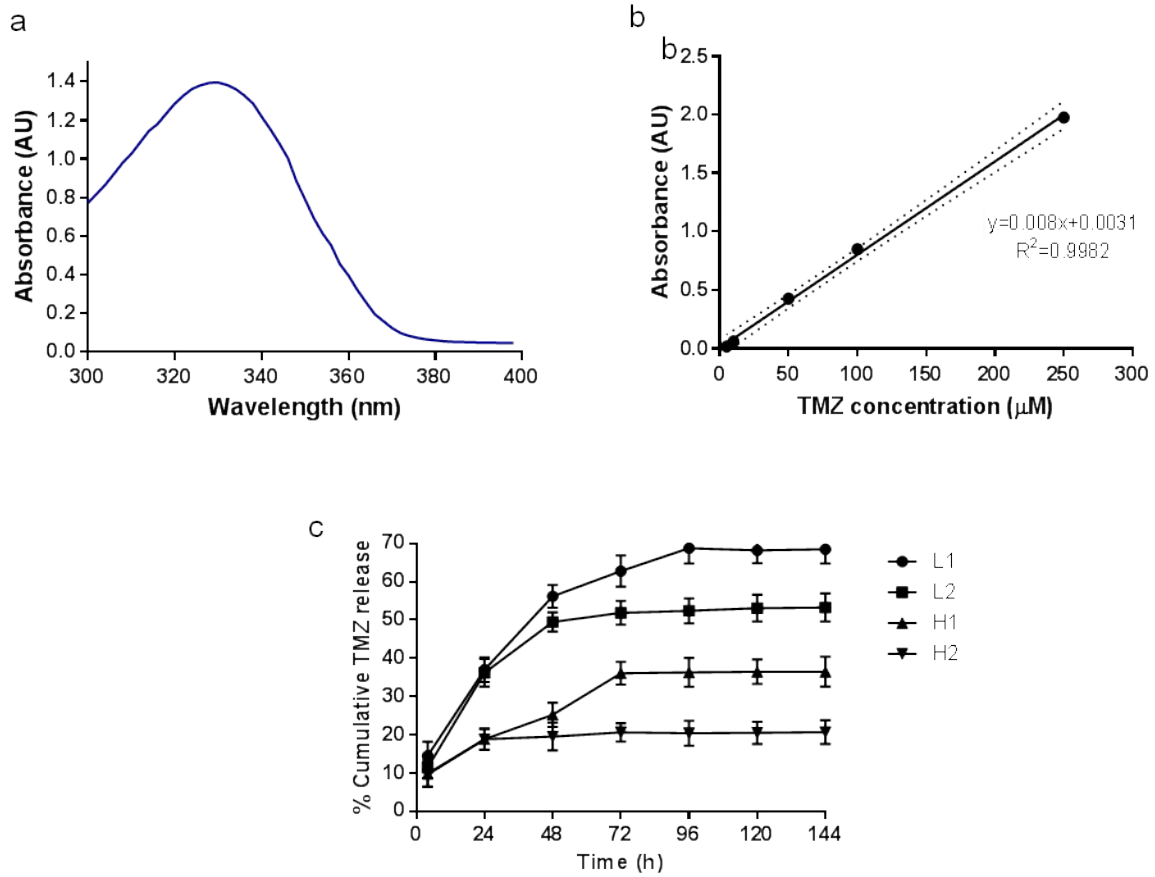

Fig. S3. a) UV/Vis spectrum of TMZ in PBS, b) calibration curve of TMZ in PBS obtained for the absorbance maximum (λ_{max}) of TMZ solution, c) Drug release profile of TMZ at 37 °C from hydrogels prepared at different crosslinking densities in PBS. The data represent the mean of triplicate conditions with the corresponding error bar calculated by standard deviation (mean ±SD).

UV-Vis absorbance/Calibration curve of FITC-hUII

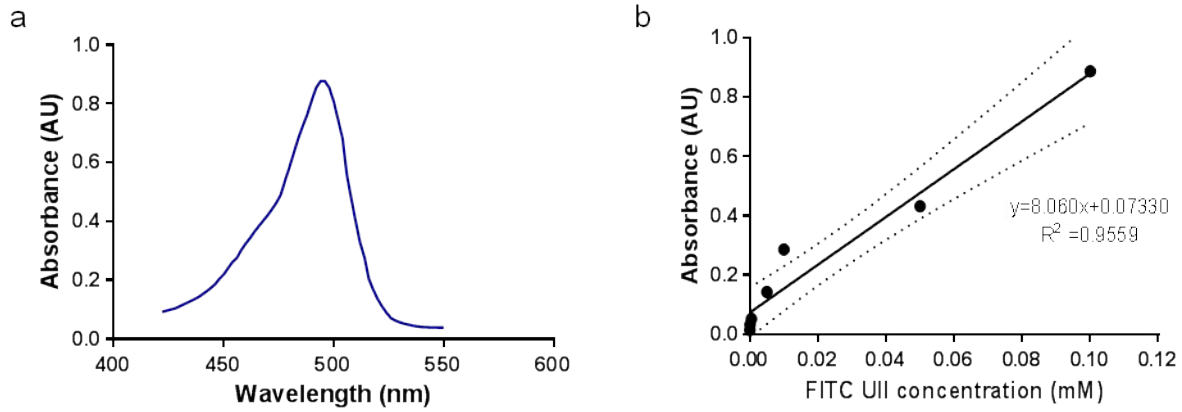

Fig. S4. a) UV/Vis spectrum of FITC-hUII in DMEM, b) calibration curve of FITC-hUII in DMEM obtained for the absorbance maximum (λ_{max}) of FITC-hUII solution.

Time sweep measurements

Time sweep measurements were conducted on an Anton Paar MCR 302 Rheometer equipped with a cylinder geometry configuration. These measurements were performed to define the gelation time for each hydrogel. Time sweep test was done with a 10 Hz frequency and a 0.1% oscillation strain at 37 °C. The rheological measurements were performed on three different samples to ensure reproducibility.

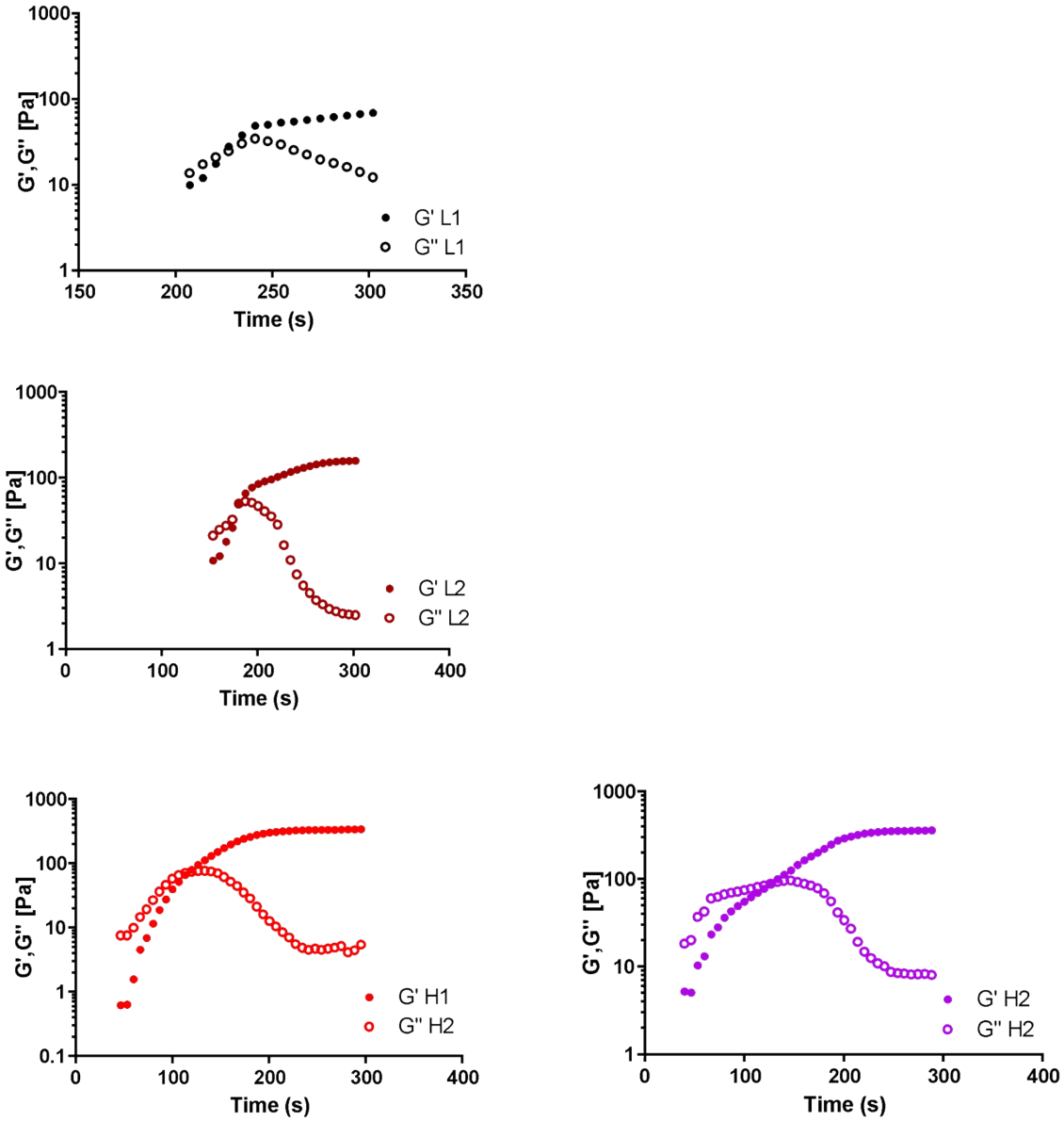

Fig. S5. Time sweep measurements of hydrogels prepared at four different crosslinking densities. The gelation time was defined for L1, L2, H1 and H2 hydrogels to be 4, 3 and 2 min respectively.

Morphology of U87MG cells on HA-ADH hydrogels

U87MG were seeded on HA-ADH scaffolds and 2D culture surfaces for 4 days. To ensure that HA-ADH hydrogels at different crosslinking densities in the absence or presence of hUII demonstrate different cell adhesive properties, the morphology of glioma cells seeded on the hydrogels was monitored as function of incubation time. As shown in Figure S5, U87MG cells presented morphology, which was highly dependent on the stiffness of the matrix. After one day of incubation, U87MG cells seeded on the standard culture surface obtained their typical elongated morphology with long cell protrusions associated with migration, whereas cells cultured on the surface of the hydrogels started to adopt rounded morphology with loss of cell adhesion. More specifically, cells seeded on the hydrogels of low crosslinking density (L1 and L2 conditions) showed rounded morphology and progressive clustering of glioma cells forming well-defined spherical shape of neurospheres, which is very typical morphology for cells seeded on soft matter. In contrast, in the case of hydrogels of high crosslinking density (H1 and

H2 conditions), cell spreading was relatively higher on the surface and cells appeared included in irregular clusters with uneven external rims and isolated, possibly due to low porosity and poor diffusion of the cell nutrients across the hydrogel network. In addition, it is noteworthy that the presence of UII had negligible effect on the morphology, shape and proliferation of glioma cells.

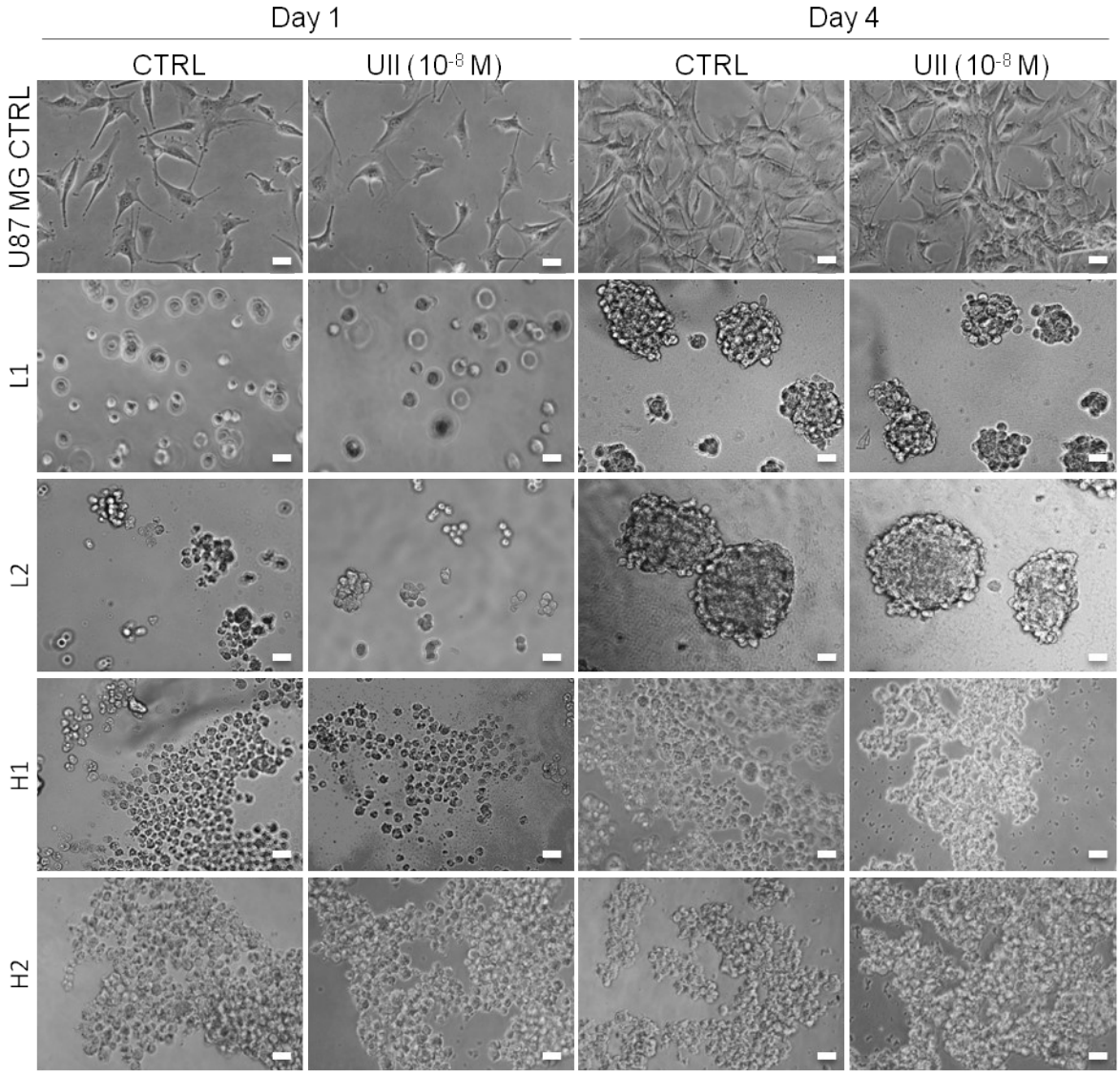

Fig. S6. Morphology of U87MG cells cultured on different crosslinking conditions of HA-ADH hydrogels in the absence or the presence of hUII (10^{-8} M). Cells were seeded onto the hydrogels for 4 days in DMEM in the absence of FBS. Representative microphotographies of cell cultures using a NIKON inverted microscope. Magnification: 20x, Scale bar: 50 µm.

Gradient or homogeneous concentration of UII on U87MG cell migration in L1 hydrogel

In order to demonstrate the gradient of the chemokine hUII ensured the directional migration of GBM cells, the cloning rings were placed vertically in each well of 24-well plate and 100 µL of HA-ADH L1 hydrogel in the absence or the presence of hUII (final concentration: 10^{-8}M) was administered into (IN) outside (OUT) or in both sides of the cloning ring. U87MG-GFP cells at 4×10^4 cells were resuspended in 500 µL of DMEM in the absence of FBS and seeded around (OUT) the cloning ring in the corresponding L1 hydrogel. After 4h polymerization, seeded cells-in-hydrogels were washed three times in DMEM to allow exchanges of DMEM and the hydrogel and the cloning rings were carefully removed by using tweezers. From D0 to D3, microphotographies of each well were taken using the Zeiss Cell Discoverer 7 microscope (PRIMACEN platform, Normandie Rouen University). Quantification of the total cell number in the well and the invasive cell number in the center void were performed by means of the Image J software. Regions of interest corresponding of the well without the ring on the one hand

and the whole of the ring on the other hand were created and the cell number was quantified by using the module “Analyze particles” from D0 to D3 after hydrogel contact. The data confirmed that a gradient concentration of hUII induced a directional invasion of the HA-ADH hydrogel while cells exposed to a homogenous concentration of hUII stopped migration and/or retained cells potentially through adhesion [3].

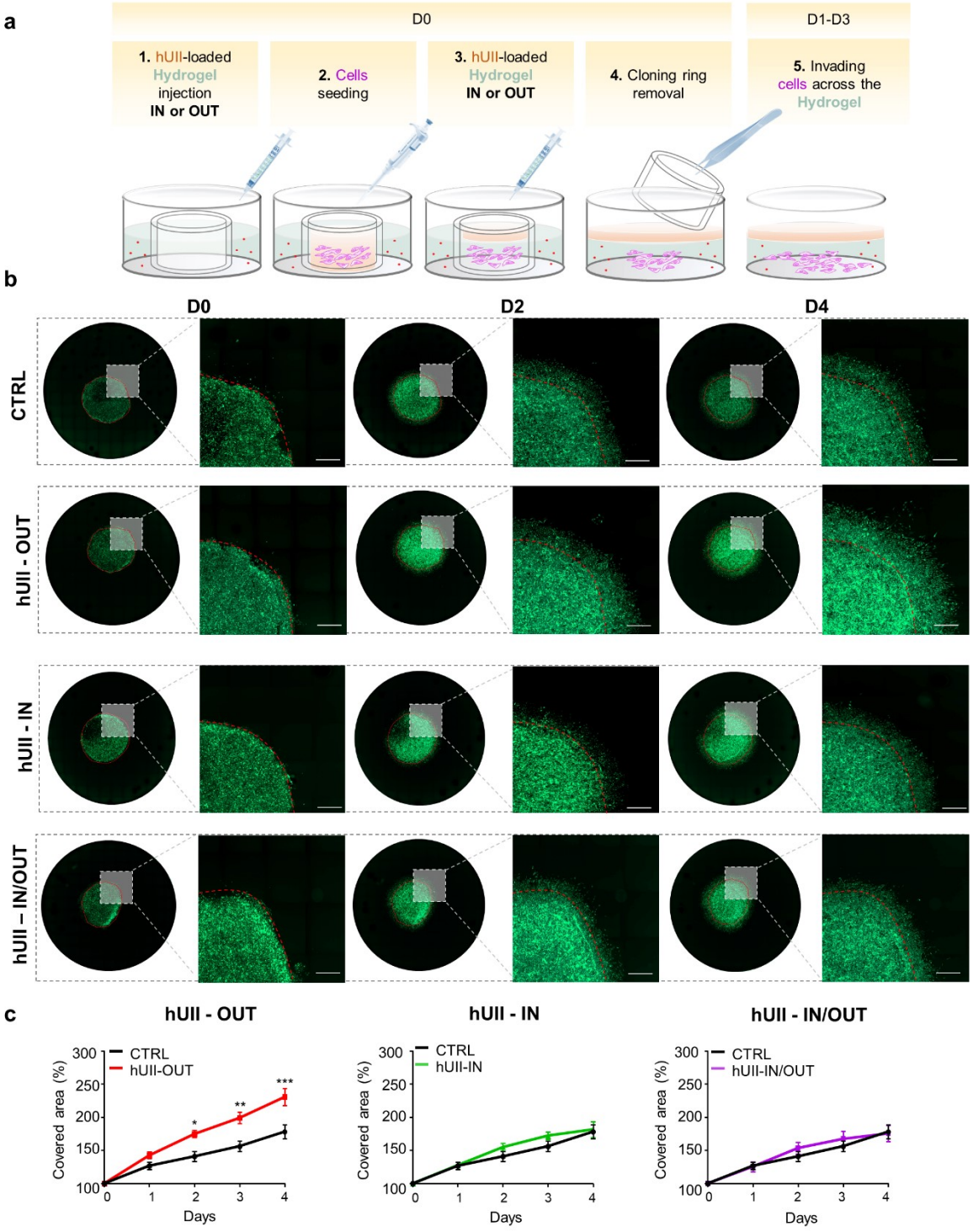

Fig. S7. a) Schematic illustration of invasion assay by using the cloning ring asay. b) Representative microphotography of U87MG-GFP cells (green) invasion at D0, D2 and D4. The seeding cells in ring central void were delineated by a dotted red circle (left image) and a zoomed image was delineated by a white square (right image). Cell invasion was evaluated by quantifying the invasion area in hydrogels loaded with DMEM (CTRL) or with hUII (10^{-8} M) added around (OUT) or into (IN) or in both sides of the cloning ring. Scale bar: 1 mm. Graphs showed the quantification of the U87MG cells invasive area in the absence or the presence of a gradient or homogenous concentration of hUII. Data were obtained from two independent

experiments in triplicate as mean with the corresponding standard deviation. Mann and Whitney test P<0.05, *; P<0.01, **; P< 000.1, ***.

Live/Dead assay on HA-ADH hydrogels

The Live/Dead assay kit (ThermoFisher Scientific) containing Calcein AM (2 µg/mL in PBS) and ethidium homodimer (4 µg/mL in PBS) reagents was prepared as per manufacturer's protocol. Briefly, U87MG cells seeded on the hydrogels and were washed with DPBS and incubated with 100 µL of Live/Dead staining solution for 25-30 minutes at room temperature. Images of the cultured cells were taken with an EVOS FLoid Cell Imaging station.

In vitro cytotoxicity of TMZ on U87MG cells

In the current work, in order to identify whether human U87MG cells are sensitive to TMZ, *in vitro* cytotoxicity assay was conducted. Briefly, glioma cells were seeded into the wells of a 96-well plate at a density of 5×10^3 cells per well and allowed to adhere overnight in DMEM. Subsequently, the cells were incubated with increasing concentrations of TMZ (50-515 µM) for 24, 48 and 72h. The stock solution of TMZ in DMSO was diluted more than 1000 times in order to prevent adverse effects on cells.

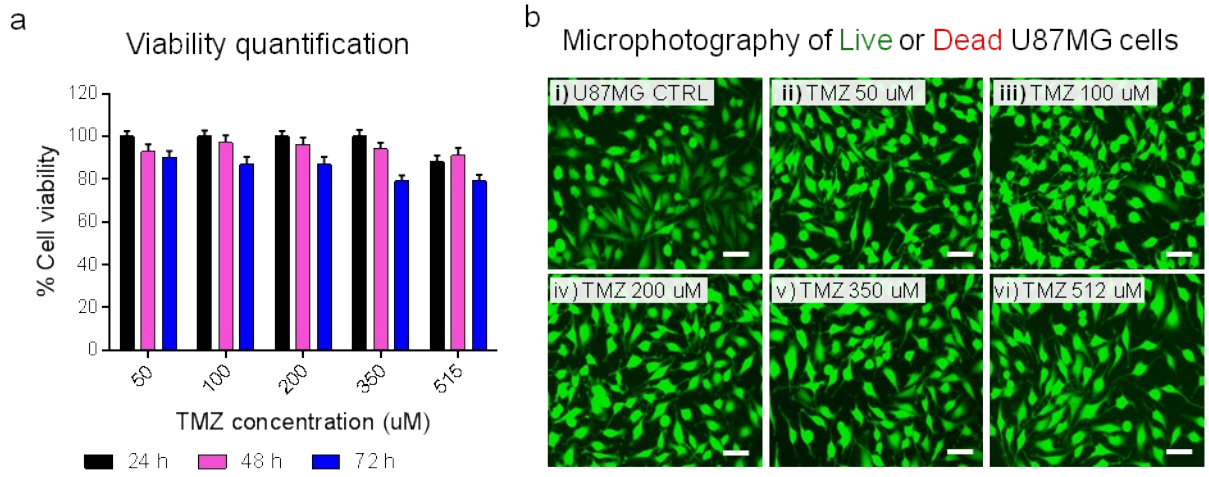

Fig. S8. a) Cell viability was measured after 24, 48 and 72h of incubation with increasing concentrations of TMZ (50-515 µM). TMZ did not induce any significant cytotoxicity on U87MG cells. All the results presented are the mean of n=6 with the corresponding error bar calculated by standard deviation, b) Representative Live/Dead photos of U87MG cells treated with increasing concentrations of TMZ after 48h of incubation i. U87MG CTRL, ii. TMZ 50 µM, iii. TMZ 100 µM, iv. TMZ 200 µM, v. TMZ 350 µM and vi. TMZ 515 µM. Magnification: 20x, Scale bar: 50 µm.

After treatment, the TMZ cytotoxicity was quantified using the MTS assay and the relative cell viability was evaluated as summarized in Figure S8. After 72 h of treatment, TMZ within the range of concentrations used, did not induce substantial cytotoxicity on glioma cells as U87MG cells presented viability >80%.

Determination of IC_{50} value for DOX on U87MG cells

U87MG cells were incubated with increasing concentrations of DOX (0.01-100 µM) for 72h and the IC_{50} concentration was determined as shown in the graph in Figure S6. It was observed that increasing concentration of DOX reduced significantly U87MG cell viability. With the range of DOX concentration employed, the IC_{50} was calculated to be ~1 µM after 72h of incubation. The IC_{50} value was defined as the concentration of DOX that caused 50% inhibition of cell growth after 72 h of treatment. In the literature, IC_{50} values for U87MG cells treated with various concentrations of DOX vary between 3.85 to 1.06 µM. [1], [2]

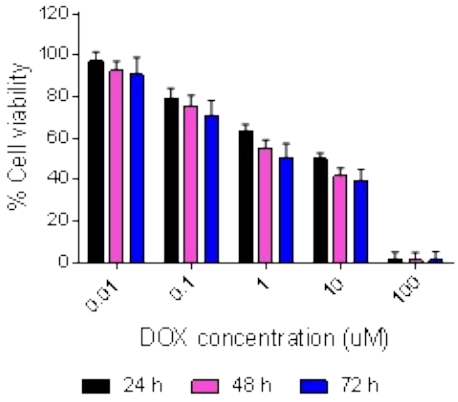

Fig. S9. *In vitro* cytotoxicity of DOX on U87MG cells. Percentage of cell viability of glioma cells after 24, 48 and 72h of treatment with increasing concentrations of DOX. The IC_{50} concentration was determined to be ~1 µM. Data represent the average of n=4 with the corresponding error bar calculated by standard deviation.

References

[1] J.F.R. Lobo, E.S. Castro, D.R. Gouvea, C.P. Fernandes, F.B. de Almeida, L.M.F. de Amorim, P. Burth, L. Rocha, M.G. Santos, L. Harmerski, N.P. Lopes, A.C. Pinto, Antiproliferative activity of Eremanthus crotonoides extracts and centratherin demonstrated in brain tumor cell lines, *Rev. Bras. Farmacogn.*, **2012**, *22*, 1295.

[2] O. Kadioglu, M. Saeed, V. Kuete, H.J. Greten, T. Efferth, Oridonin Targets Multiple Drug-Resistant Tumor Cells as Determined by in Silico and in Vitro Analyses, *Front Pharmacol.*, **2018**, *9*, 355.

[3] C. Lecointre, L. Desrues, J.E. Joubert, N. Perzo, P.O. Guichet, V. Le Joncour, C. Brulé, M. Chabbert, R. Leduc, L. Prézeau, A. Laquerrière, F. Proust, P. Gandolfo, F. Morin, H. Castel, Signaling switch of the urotensin II vasosactive peptide GPCR: prototypic chemotaxic mechanism in glioma, *Oncogene*, **2015**, *34*, 5080.